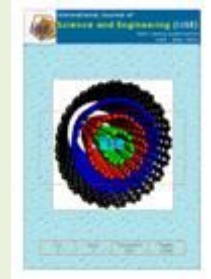




International Journal of Science and Engineering (IJSE)

Home page: <http://ejournal.undip.ac.id/index.php/ijse>



Turbidity Measurement Using An Optical Tomography System

Sallehuddin Ibrahim, Mohd Amri Md Yunus, Mohd Taufiq Mohd Khairi

Faculty of Electrical Engineering, University Teknologi Malaysia, Skudai, Johor 81310, Malaysia
Corresponding Author: salleh@fke.utm.my

Abstract - Turbidity is used to describe water quality and it can be caused by the presence of suspended particles and organic matter such as algae, clay and silt. The measurement of turbidity level of water is vital to domestic water supplies since it is related to public health and water treatment process. This paper presents an investigation on an optical tomography system to estimate the turbidity level in a sample of water. The optical sensors consist of infrared light-emitting diodes (LED) as transmitters and photodiodes as the receivers where the projections of the sensors are designed in fan beam mode. The system was tested using a vertical flow pipe. The Independent Component Analysis (ICA) method was used to display the concentration profile. Results obtained proved that the technique can provide the concentration profile representing the turbidity level of water.

Key words - ICA; optic; process; tomography; turbidity

Submission: September 17, 2013

Corrected: October 6, 2013

Accepted: October 8, 2013

Doi: [10.12777/ijse.5.2.66-72](https://doi.org/10.12777/ijse.5.2.66-72)

[How to cite this article: Ibrahim, S., Yunus, M.A.M. and Khairi, M.T.M. (2013). Turbidity Measurement Using An Optical Tomography System. International Journal of Science and Engineering, 5(2),66-72. Doi: [10.12777/ijse.5.2.66-72](https://doi.org/10.12777/ijse.5.2.66-72)]

Introduction

Environmental pollution has reached a level which caused many people to be worried. It does not only caused our health to be affected but it also lead to deaths. This is due to the fact that industrialization is running at a rapid pace and the environmental regulations in many countries are not strict enough to curb such pollution from harming mankind. Currently there is an extensive research on measuring and removing pollution such as those in water and the atmosphere. For the survival of mankind, a reduction in pollution is vital and as such investigation on techniques to measure and remove pollution is being conducted widely throughout the world (Wilde, 1998). Turbidity is one way of measuring the level of environmental pollution. Turbidity is a measurement of how cloudy or clear the water is, or, how easily light can be transmitted through it. Scientists often relates water turbidity in with other factors so as to comprehend its causes and consequences. As an example, high levels of turbidity can identify problems with erosion, reduction in water quality, decreased light penetration diminished recreational values and aesthetics as well as direct and indirect effect on fish, invertebrates, aquatic plants (Kerr, 1995)

By carrying out analysis on turbidity, the optical characteristics that resulted in light through water to be

scattered and absorbed rather than transmitted in straight paths can be investigated. When light is projected onto water, the particles in water will block light from being transmitted through water. If water is pure, light will be transmitted without any interruption, with slight scattering. Various factors such as the size, shape and composition of the particles will influence the interaction between light and suspended solids. Particles also absorb and attenuate light (Omar *et al.*, 2009). There will be changes in the direction of the light path when it hits the particles.

Tomography is a means of determining the internal characteristics of a flow region or a cross-section of an object from which local information such as volume fraction and velocity can be extracted (Ibrahim, 2002). The discovery of X-rays by Conrad Röntgen in 1895 inspired the development of computed tomography. The motivation for this development was in the medical field. The clinicians are not satisfied with planar X-radiographs and so they demanded the radiologists to supply them with tomographic images. Hounsfield developed and commercialized the first axial computer tomography in 1972 known as the EMI-Scanner. In 1974 research in tomography received a boost when the first images of a

living subject were published (Seynaeve et al., 1995). Today tomography continues to make significant process drawing a lot of interest from many researchers and is being used for various applications.

Optical tomography is a powerful method which can be applied for combustion diagnostics, deliverance of the spatial distributions of gas concentration, absorption and refractive index, emissivity, density and temperature without invading the object of interest (Schwarz, 1996). Optical tomography has the advantages of being non-invasive and non-radiative as compared to other techniques. Tomographic imaging of the contents of a flowpipe focuses on the computation of a pseudo cross-section from a set of optical measurements obtained from surrounding optical sensors. Optical tomography can be utilized to provide the concentration profile of the turbidity level of various multi-phase mixture.

In order to display the concentration profiles, the Independent Component Analysis (ICA) method was used. Historically, ICA was introduced in 1990 with the purpose of separating independent source variable from a linear mixture and it is through this method the mixed signal problem can be solved. The benefit of ICA is that it is statistically independent and distributed in a non-Gaussian manner as compared to other methods such as Principal Component Analysis (PCA) and Factor Analysis (FA) (Wang et al., 2008). In this project, ICA was used to separate the signals detected by the light receivers. This technique can be expressed by the following expression,

$$Y = MS \tag{1}$$

In which Y is n x m matrix representing the mixture of source signals, M is n x d matrix which represents the mixing matrix, and S is d x m matrix representing the

source signal. Initially the separating matrix P is determined in which

$$P = M^{-1} \tag{2}$$

Finally the each source can be obtained from the following expression,

$$S = PY \tag{3}$$

Modelling

The arrangement of light transmitters and receivers in the pipe is shown in Fig. 1. Transmitters are denoted as TX whereas receivers are denoted as RX. Light is transmitted in the form of fan-beam projection mode. The circle represents the pipe. The fan beam projection is projected onto a sensitivity map having 18 x 18 pixels. Consider receiver 1. Ideally, light from all transmitters arrived at receiver 1 which is denoted as RX1. However results obtained from an earlier investigation (Mohd Khairi et al., 2013) showed that signals from only four transmitters are significant compared to the other transmitters. These four signals have a magnitude of 3.7V as observed by an oscilloscope. The transmitters which transmit these signals are transmitters 9, 10, 11 and 12 which are located diametrically opposite to receiver 1. Similarly measurement showed that for the other receivers, only four transmitters transmit light which can be significantly detected by each receiver as shown in Table 1. The ICA technique is then used to distinguish each signal which is detected by the receiver and subsequently the ICA method was utilized to obtain the matrices which contain the value of the turbidity factor (T).

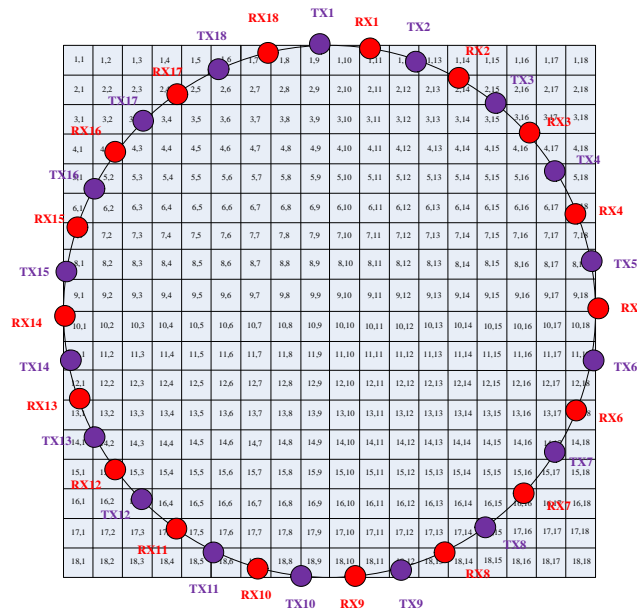


Figure 1. Optical system configuration around the pipe

Table 1. Result of transmitters detected by receivers

Receiver	Transmitter
1	9, 10, 11, 12
2	10, 11, 12, 13
3	11, 12, 13, 14
4	12, 13, 14, 15
5	13, 14, 15, 16
6	14, 15, 16, 17
7	15, 16, 17, 18
8	16, 17, 18, 1
9	17, 18, 1, 2
10	18, 1, 2, 3
11	1, 2, 3, 4
12	2, 3, 4, 5
13	3, 4, 5, 6
14	4, 5, 6, 7
15	5, 6, 7, 8
16	6, 7, 8, 9
17	7, 8, 9, 10
18	8, 9, 10, 11

Light is attenuated as it propagates from one medium to another. In accordance with the Beer-Lambert's law, the intensity of light will be reduced as it arrived at the light receiver as a result of attenuation by the medium. The attenuation of light is based on the Beer-Lambert law which can be expressed as follows:

$$M = \begin{pmatrix} \exp(-\alpha 2L1) & \exp(-\alpha 2L1) & \exp(-\alpha 3L2 - \alpha 2L3) & \exp(-\alpha 1L2 - \alpha 2L3) \\ \dots & \dots & \dots & \dots \\ \dots & \dots & \dots & \dots \\ \dots & \dots & \dots & \dots \end{pmatrix} \tag{7}$$

In order to separate the original signal, the ICA algorithm is utilized. The separating matrix P is the parameter of interest. In ICA, the rows of matrix P have to be rearranged based on the transmitters' sequence as P can only separate the signal but the as a result the matrix is randomly located. Taking into account of this, the pulse duration of each transmitter is set differently from each other.

Hardware And Software

The optical tomography system (Fig. 3) consists of optical sensors which are placed around a pipe, a signal conditioning circuit, a data acquisition system and image reconstruction. To enable such a system to display

$$Z = \ln\left(\frac{V_2}{V_1}\right) = -\alpha l \tag{4}$$

where Z is the medium absorbance, V₂ is the resultant sensor voltage, V₁ is the voltage of the receiver without any attenuation, α is the absorption coefficient and l is the length of the medium. For pure water the attenuation coefficient is 0.0287/mm. When pure water is contaminated, the value of the attenuation coefficient will change. The level of turbidity can be observed in the mixing matrix M which contains the exp(-αl) components.

Independent Component Analysis

Only four sets of sensors are chosen in order to simplify modelling. Consider light arriving at receiver 1 as shown in Figure 2 which is a mixture of signals from four transmitters. Light from TX1 and TX2 (which are adjacent to RX1) are transmitted directly to RX1. Light from TX3 is a combination of attenuation and length involving (α₃l₂) and (-α₂l₃). Light from TX4 is a combination of attenuation and length involving (α₁l₂) and (α₂l₃). Hence the equation describing the relationship between light from four transmitters to receiver 1 can be expressed as:

$$V_{RX1} = V_{TX1}e^{(-\alpha 2L1)} + V_{TX2}e^{(-\alpha 2L1)} + V_{TX3}e^{(-\alpha 3L2 - \alpha 2L3)} + V_{TX4}e^{(-\alpha 1L2 - \alpha 2L3)} \tag{5}$$

Equation (1) can be simplified as

$$V_{RN} = MV_{TN} \tag{6}$$

where V_{RN} represents the mixture of source signals V_{RX1}, V_{RX2}, ..., V_{RX18}; V_{TN} represents the source signals V_{TX1}, V_{TX2}, ..., V_{TX18} and the mixing matrix, M, can be expressed as

accurately images of the concentration profile in the flow pipe, the geometrical configuration of the sensors must be carefully selected.

The main component at the forefront of the measurement system is the optical sensors. This project made use of eighteen TSAL6200 infrared light-emitting diodes which are used as light transmitters and eighteen BPV10NF photodiode receivers. The sensors are installed around a 100 millimetres (mm) diameter transparent pipe. LEDs are selected as light transmitters in order to prevent the surrounding light from affecting the optical system.

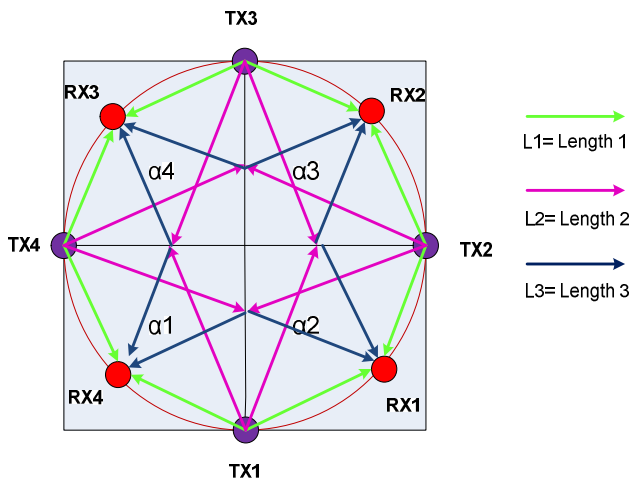


Figure 2. Light paths

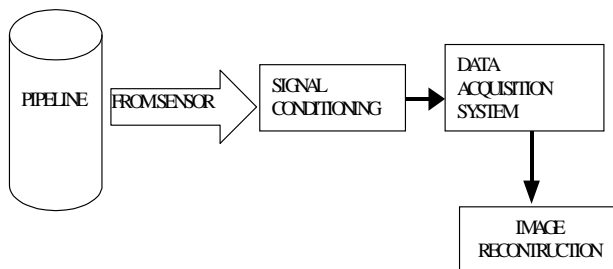


Figure 3. Optical tomography system

This is due to the fact that infrared is invisible light, which has a smaller wavelength of 750 nm in comparison to the wavelength of visible light which has a wavelength of about 380 nanometres. Each transmitter has been programmed by a PIC microcontroller is used to program each transmitter so that it can generate different pulse durations. The purpose of doing this is to identify which transmitters' signals have been detected by the receiver. In the signal conditioning circuit the first stage performs the task of converting light to voltage. The

output voltage as a result of this conversion is however small and hence the subsequent stages of the signal conditioning circuit play the role of amplifying the voltage. The analog output from the signal conditioning unit is digitized by an U2331 data-acquisition system (DAQ) manufactured by Agilent Technologies. The software used to perform ICA is the LabVIEW software developed by National Instruments as shown in Fig. 4. The eighteen output of receivers (box 1) are inputted to the ICA block (box 2). The ICA produced separating matrix (box 3) in the form of an 18 x 18 matrix and recovered the signal. The matrix's size depends on the number of inputted in the ICA. For example, if ICA received four inputs from receiver, hence the separating matrix will be a 4 x 4 matrix. In ICA, the square method is utilised since it can recover the signal better compared to tanh, gaussian, and cube. The recovered signals are vital in rearranging the matrix row as required.

The software has been chosen since it contains the tools to perform ICA in the form of object programming. This eliminates the task of creating a new programming code. The FastICA algorithm is used in this Project. It is an efficient and well-known algorithm for ICA developed by Aapo Hyvärinen at Helsinki University of Technology (Hyvärinen, 1999). Initially, the ICA was used to separate the four signals detected by each receiver. Secondly, the ICA results in the improper arrangement of the matrix. As such, the matrix has to be rearranged in which the row in the matrix should be arranged at the appropriate row based on the value of pulse duration. This resulted in the mixing matrix M . Thirdly, the ICA also resulted in the separating matrix P . The inverse matrix (M^{-1}) contains the exponential component $\exp(-\alpha)$ or termed the turbidity matrix. In order to obtain the individual signals, the LabVIEW software is chosen since it has the ICA function. Information on the values of pulse duration is obtained automatically by LabVIEW using the "timing and transition measurement" tool.

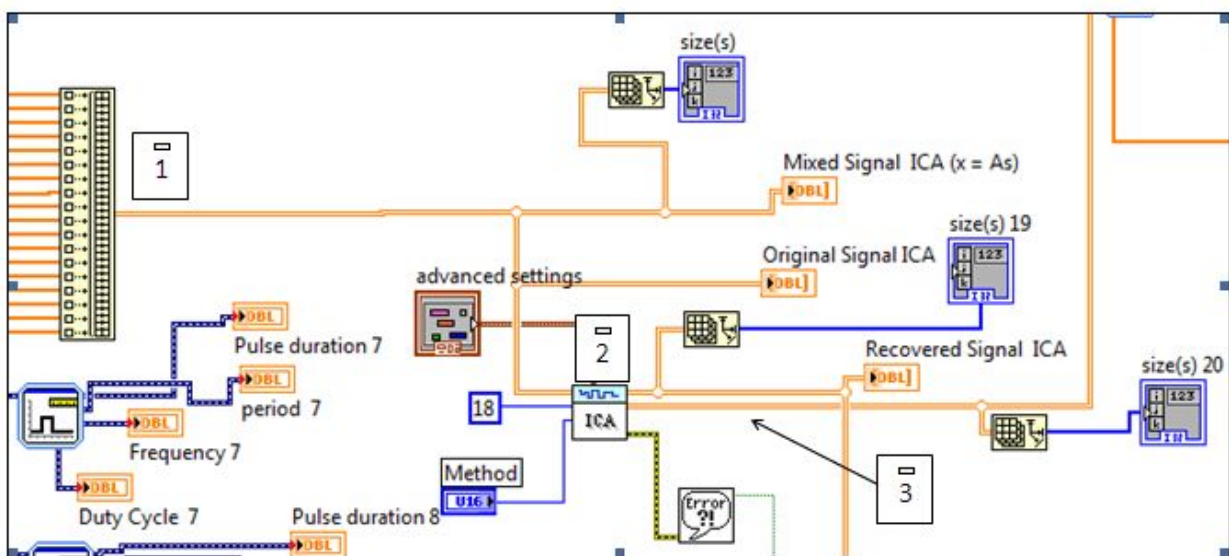


Figure 4. LabVIEW program which incorporates ICA

Results and Discussion

Several experiments were carried out to test the tomography system using the ICA method. The experiments involved pure and contaminated water. Initially, the transparent pipe was filled with 3 litres of pure water. Measurement of pulse duration was obtained

using LabVIEW. Based on the measurement result, the rows in the matrix will be rearranged based on the value of pulse duration. For pure water, the average values representing the concentration profile is shown in Figure 5.

																Average Value (K)	
0	0	0	0	0	0.1989	0.2305	0.1873	0.1279	0.1756	0.1561	0.1388	0.1352	0	0	0	0	0
0	0	0	0.08141	0.2823	0.13	0.1089	0.1073	0.0679	0.0674	0.0969	0.1141	0.1376	0.1233	0.1771	0	0	0
0	0	0.0811	0.15	0.0986	0.0631	0.0476	0.0386	0.0526	0.0666	0.0516	0.0514	0.0759	0.0707	0.1028	0.1371	0	0
0	0.0672	0.1214	0.0701	0.0662	0.0666	0.0479	0.0406	0.0406	0.0479	0.0276	0.0533	0.0493	0.0572	0.0544	0.085	0.0546	0
0	0.1783	0.0717	0.0642	0.0286	0.0479	0.0492	0.0422	0.0357	0.0331	0.0246	0.0461	0.027	0.0462	0.0407	0.0521	0.0689	0
0.1716	0.0538	0.0504	0.0417	0.0299	0.0467	0.0557	0.0414	0.0371	0.0554	0.0504	0.0328	0.0449	0.0252	0.0478	0.0578	0.057	0.04
0.0664	0.0481	0.0515	0.0344	0.036	0.0345	0.05	0.0406	0.0639	0.0434	0.0383	0.0497	0.0325	0.0515	0.0404	0.0313	0.0582	0.0772
0.0638	0.0336	0.0556	0.0518	0.0386	0.0438	0.0582	0.0501	0.0419	0.0353	0.0472	0.0343	0.0329	0.0453	0.0369	0.0325	0.0348	0.072
0.0648	0.0536	0.0537	0.05	0.0483	0.0589	0.0494	0.0512	0.0676	0.0343	0.05	0.0303	0.0451	0.0401	0.0341	0.0397	0.0504	0.0724
0.0693	0.0753	0.0477	0.0426	0.0485	0.0599	0.0333	0.0625	0.0171	0.0457	0.0345	0.0401	0.0424	0.0377	0.0463	0.0365	0.0405	0.0971
0.0614	0.078	0.0596	0.0498	0.0342	0.0333	0.0378	0.0489	0.0378	0.0407	0.0375	0.0331	0.037	0.0386	0.043	0.0445	0.0357	0.0861
0.1008	0.0673	0.063	0.0365	0.0275	0.0353	0.0402	0.0416	0.0482	0.0293	0.0382	0.0412	0.0382	0.0472	0.0452	0.045	0.0517	0.1349
0.1327	0.0713	0.0491	0.0355	0.0357	0.0276	0.039	0.0345	0.046	0.0343	0.0445	0.0437	0.0478	0.032	0.0447	0.0653	0.0569	0.0718
0	0.0751	0.0524	0.0733	0.0397	0.0471	0.0486	0.0286	0.0457	0.051	0.0436	0.0357	0.0465	0.0508	0.0452	0.0477	0.1096	0
0	0.0455	0.0535	0.0476	0.0553	0.0761	0.04	0.0369	0.0356	0.0518	0.0489	0.0443	0.0391	0.0582	0.046	0.0473	0.0272	0
0	0	0.0465	0.0489	0.0433	0.0512	0.0566	0.0539	0.0425	0.0447	0.062	0.0435	0.0558	0.0408	0.0553	0.0232	0	0
0	0	0	0.0323	0.0912	0.0625	0.0479	0.0483	0.0711	0.0666	0.0492	0.0421	0.0529	0.0996	0.0337	0	0	0
0	0	0	0	0.0664	0.0823	0.1094	0.0671	0.0729	0.1772	0.1421	0.0613	0	0	0	0	0	0

Figure 5. The numerical concentration profile for pure water

Several experiments were performed which made use of three litres of pure water contaminated with 25 ml green coloring which is used as food coloring as shown in Figure 6. The green color resembles algae which is one of the contaminants normally found in contaminated water. As a result of applying ICA, the concentration profile is obtained as shown in Figure 8.

of calculation of the pixel values for the concentration profile is shown in Table 2.

A comparison of the numerical profiles of pure water (Figure 6) and contaminated water (Figure 7) shows that the numerical values in each pixel in the contaminated water concentration profile is higher than that of pure water. This occurred as a result of light experiencing more attenuation when it traversed the contaminated water. Mathematically this can be explained by the fact that the mixing matrix M contains the exponential component $\exp(-\alpha l)$. So when the attenuation coefficient (α) is reduced the value of $\exp(-\alpha l)$ increased. Due to the limitation of the ICA method, values of the pixels near the pipe wall are higher than the rest of the pixels. This can be explained by the fact that the transmitters and receivers are located at the pipe wall and hence light accumulated near the pipe wall. Examples

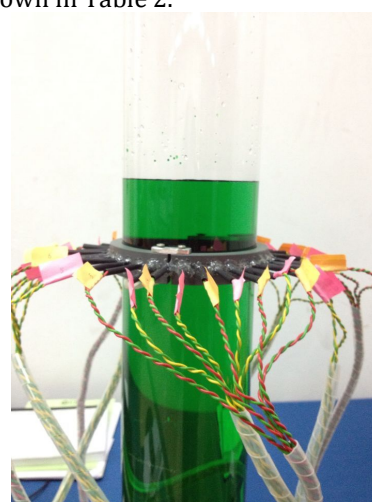


Figure 6. Contaminated water

Table 2. The calculation of average values for pixels (1,9) and (1,10) in contaminated water

Pixel	Sum of pixels	Numerical sum of pixels	Total	Number of pixels traversed by light	Average Value
1,9	$M_{1,1} + M_{18,1} + M_{17,1} + M_{16,1} + M_{1,3} + M_{1,4} + M_{1,5} + M_{1,2} + M_{1,6} + M_{1,7} + M_{1,8} + M_{1,9} + M_{1,10} + M_{1,11} + M_{1,12} + M_{1,13} + M_{1,14} + M_{1,15} + M_{1,16} + M_{1,17} + M_{2,17} + M_{1,18} + M_{2,18} + M_{3,18} + M_{4,18}$	0.4906 + 0.0736 + 0.0279 + 0.0299 + 0.0623 + 0.0153 + 0.0057 + 0.0154 + 0.0381+ 0.0203 + 0.1006 + 0.0075 + 0.1063 + 0.0366 + 0.1811 + 0.0776 + 0.2049 + 0.7765 + 0.1411 + 0.0307 + 0.0887 + 0.0799 + 0.0696 + 1.1693 + 0.8872	4.7375	25	0.1895
1,10	$M_{1,1} + M_{18,1} + M_{17,1} + M_{16,1} + M_{15,1} + M_{14,1} + M_{13,1} + M_{12,1} + M_{1,2} + M_{1,3} + M_{1,4} + M_{1,5} + M_{1,6} + M_{1,7} + M_{2,7} + M_{2,18} + M_{3,18}$	1.2265 + 0.2208 + 0.0836 + 0.0697 + 0.1039 + 0.0153 + 0.0019 + 0.0267 + 0.0435 + 0.0673 + 0.4130 + 0.2088 + 0.9744 + 0.8872 + 0.2352 + 0.0307 + 0.0887	4.6971	17	0.2763

																	Average Value (K)	
0	0	0	0	0	0	0.2996	0.336	0.2126	0.1895	0.2763	0.1601	0.0543	0.0733	0	0	0	0	0
0	0	0	0.2519	0.6999	0.2288	0.2096	0.1533	0.1056	0.0976	0.1008	0.0836	0.0809	0.0774	0.1402	0	0	0	0
0	0	0.4269	0.3944	0.1658	0.1517	0.1029	0.0993	0.0856	0.0778	0.0651	0.0633	0.0696	0.068	0.0739	0.0931	0	0	0
0	0.2032	0.3925	0.1221	0.1198	0.1588	0.0803	0.0682	0.1083	0.0921	0.0369	0.0905	0.0671	0.0369	0.0327	0.0648	0.0414	0	0
0	0.3302	0.2017	0.1092	0.1352	0.0812	0.0908	0.0648	0.0562	0.055	0.0739	0.1324	0.0395	0.0726	0.0488	0.054	0.0747	0	0
0.7355	0.2113	0.1185	0.1125	0.1096	0.0467	0.1037	0.0654	0.0694	0.1058	0.0704	0.088	0.0917	0.0567	0.0693	0.059	0.0644	0.0564	0
0.4257	0.1971	0.0677	0.0744	0.1224	0.0453	0.0738	0.0673	0.0603	0.0587	0.0409	0.0762	0.0635	0.0799	0.069	0.0667	0.0516	0.0849	0
0.3688	0.1151	0.114	0.1202	0.0875	0.0705	0.0754	0.0744	0.0601	0.0329	0.0666	0.0343	0.0716	0.0633	0.0601	0.0794	0.0775	0.0973	0
0.2569	0.1159	0.0659	0.1432	0.106	0.0957	0.0844	0.0587	0.0792	0.051	0.0845	0.0602	0.0821	0.0395	0.0483	0.0726	0.1174	0.122	0
0.3432	0.151	0.0498	0.0734	0.1076	0.1108	0.031	0.0627	0.0208	0.07	0.0389	0.0774	0.0872	0.0597	0.0717	0.0474	0.0672	0.1598	0
0.1747	0.112	0.0877	0.0911	0.0787	0.065	0.1042	0.0692	0.0477	0.0408	0.0737	0.0632	0.0815	0.0541	0.0461	0.0522	0.0461	0.1151	0
0.2358	0.1038	0.0839	0.0696	0.284	0.0547	0.0627	0.0816	0.0799	0.0518	0.0439	0.0703	0.0631	0.0702	0.0526	0.0621	0.0824	0.0784	0
0.1947	0.1177	0.0695	0.0885	0.1024	0.0652	0.101	0.0838	0.0765	0.096	0.0596	0.0522	0.0734	0.0828	0.0471	0.0757	0.0615	0.0513	0
0	0.1585	0.0591	0.1108	0.0939	0.0865	0.0687	0.0518	0.0976	0.0783	0.122	0.0652	0.0699	0.0933	0.0452	0.1029	0.1037	0	0
0	0.1662	0.0899	0.0989	0.0781	0.0504	0.0617	0.0863	0.0794	0.0824	0.0481	0.0945	0.0788	0.1102	0.0684	0.1015	0.0429	0	0
0	0	0.0405	0.125	0.0876	0.0785	0.0453	0.037	0.0466	0.0439	0.056	0.0553	0.1024	0.1143	0.1726	0.0832	0	0	0
0	0	0	0.1473	0.311	0.1123	0.0911	0.0691	0.0777	0.0803	0.0782	0.0756	0.1012	0.1534	0.1004	0	0	0	0
0	0	0	0	0	0.0712	0.0682	0.1136	0.0926	0.0961	0.1281	0.0958	0.0393	0	0	0	0	0	0

Figure 7. Numerical concentration profile of contaminated water

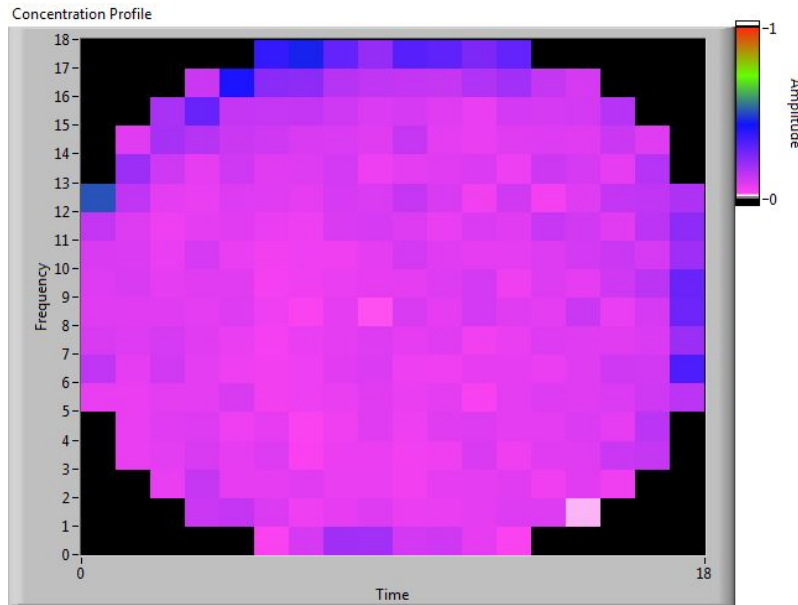


Figure 8. Concentration profile of contaminated water

Conclusions

The concentration profile of the turbid liquid depends on the intensity and the pattern on the light projected through the liquid as well as the liquid tendency to absorb certain wavelengths of the incident light. When water is pure or clear, there is almost no interruption of light from the transmitters to the receivers. In turbid water, light will be attenuated. The tomography system can provide the concentration profile of both pure and contaminated water which can be used to show the level of turbidity. By knowing the turbidity level, problems such as erosion at shoreline could be identified and thus costly economic and environmental impacts can be avoided. Further experiments will be carried out on other types of contaminants to test the effectiveness of the system.

Acknowledgments

The authors wish to acknowledge the assistance of the Malaysian Ministry of Higher Education and Universiti Teknologi Malaysia under the GUP Research Vote 08J73 for providing the funds and resources in carrying out this project.

References

Hyvärinen A. (1999) Fast and Robust Fixed-Point Algorithms for Independent Component Analysis. *IEEE Transactions on Neural Networks* 10(3):626-634; <http://www.cs.helsinki.fi/u/ahyvarin/papers/TNN99new.pdf>

Ibrahim, S. (2002), Investigation on Optical Fibre Configurations for Process Tomography, *Jurnal Teknologi*, 36(D): 35-46; <http://eprints.utm.my/1393/1/JT36D3.pdf>

Kerr, S. J. (1995) Silt, Turbidity and Suspended Sediments in the Aquatic Environment: An Annotated Bibliography and Literature Review, Ontario Ministry of Natural Resources, Southern Region Science & Technology Transfer Unit Technical Report TR-008, Ontario, Canada; <http://www.mnr.gov.on.ca/stdprodconsume/groups/lr/@mnr/@letsfish/documents/document/228131.pdf>

Mohd Khairi, M. T., Ibrahim, S., Md Yunus, M. A., Mohd Sulaiman, M. N. (2013). Optical Tomography Sensor Configuration for Estimating the Turbidity Level of Water. *Proceedings of the International Graduate Conference Engineering, Science and Humanities*, Apr. 16-17, Universiti Teknologi Malaysia, Johor, Malaysia.

Omar, A.F. and Mat Jafri, M.Z. (2009). Turbidimeter Design and Analysis: A Review on Optical Fiber Sensors for the Measurement of Water Turbidity. *Sensors*, 9(10): 8311-8335; <http://www.mdpi.com/1424-8220/9/10/8311>

Schwarz A. (1996). Multi-tomographic Flame Analysis With a Schlieren Apparatus, *Measurement Science and Technology*, 7: 406; <http://iopscience.iop.org/0957-0233/7/3/023>

Seynaeve, P.C. and Broos J.I. (1995). The History of Tomography. *Journal Belge de Radiologie*, 78: 284-288; <http://www.ncbi.nlm.nih.gov/pubmed/8550391>

Wang, G., Ding, Q. and Hou, Z. (2008). Independent Component Analysis and Its Applications in Signal Processing for Analytical Chemistry. *Trends in Analytical Chemistry*, 27: 368-376; <http://www.sciencedirect.com/science/article/pii/S0165993608000101>

Wilde, F. D. and Gibs, J. (1998). *Turbidity*, U.S. Geological Survey TWR1 Book 9, No. 4; <http://water.usgs.gov/owq/FieldManual/Chapter6/Section6.7.pdf>